Test-to-Failure of a Jack-Arch Bridge

DAVID B. BEAL

ABSTRACT

A 76-year-old jack-arch bridge was tested to failure to obtain information on load capacity and the degree of composite action between the steel beams and concrete deck. This work was started because, despite the good condition of the majority of the 1,300 jack-arch bridges in New York, load-rating estimates indicated that they were inadequate to support modern highway traffic. The most likely explanation for the observed performance of these bridges is that they are resisting loads in ways not considered in design or load-rating calculations. Although these bridges have no mechanical shear-transfer devices to assure composite action, it was suspected that chemical bond and friction were sufficient to provide the observed enhancement in load capacity. The 39-ft-span test structure consisted of six 24-in.-deep I-beams spaced at 36 in. Instrumentation consisted of electrical resistance strain gauges on both flanges at midspan, end rotation measurement devices at the ends of two beams, and deflectometers at midspan. The bridge was loaded to produce a 6-ft region of constant moment at the center of the span. Loads were applied through hydraulic jacks reacting against grouted anchors beneath the structure. It is concluded that full composite action may be assumed in load-rating estimates of jack-arch bridges. Although significant restraint of end rotation was also observed in both tests, a generalization of this restraint to other structures is not possible.

BACKGROUND

Jack-arch bridges are a small but important component of New York State's highway bridge population. More than 1,300 of these bridges, constructed between 1920 and 1940, are currently in service on state and local highway systems. These normally short-span bridges were constructed with steel beams encased in concrete. Curved sheets of corrugated metal, supported on the lower flanges of the beams, were used to form the concrete, producing the "arches." In some structures the lower flange of the beam was also encased in concrete in a separate pour, but this detail is not inherent to the structural form.

In many cases present load capacity of jack-arch bridges is estimated to be less than that required to support modern traffic. This deficiency is not unexpected because the design live load was only 20 tons, in contrast to the 40-ton trucks that are now legal. In addition, frequent pavement overlays have increased the dead load to a level that leaves many structures with little apparent remaining capacity to resist traffic. The difficulty of determining condition of the concrete-encased steel member increases the conservatism of the load rating and thus contributes to low estimates of load capacity.

Despite these apparently justified low load-capacity estimates for jack-arch bridges, many are in good condition and are carrying modern highway loads without distress after many years of service. The most likely explanation for the observed performance of these bridges is that they are resisting loads in ways that were not anticipated during design and that are not now considered in load-rating calculations. At the time jack-arch bridges were being designed, for example, composite action (the steel and concrete participating together in resisting traffic loads and dead loads other than the concrete itself) was not considered. In general, it was not until the 1950s that composite behavior was included in bridge design calculations. Bridges do not behave compositely just because the designer decides to include such behavior in calculations. In modern construction, a mechanical connection is required between the concrete and steel before composite action can be assumed. Jack-arch bridges, of course, have no mechanical connections and thus cannot be assumed to be composite without experimental justification.

Despite the lack of shear connectors, ample evidence exists that composite action is achieved in many structures. In a test of a truss-bridge floor system (1) the magnitude of the measured strains resulting from application of the test load could be explained only by assuming composite behavior. Unintentional mechanical and chemical bond between the materials provides resistance to slip and permits development of partial composite action at service loads.

It was recognized that, if composite action is actually achieved in jack-arch bridges, the increase in calculated load capacity would be sufficient, in the majority of cases, to remove all load restrictions. The purpose of the work described in this paper was to determine experimentally the magnitude of composite action, if any, achieved in jack-arch bridges under service loads and under loading to failure.

In an earlier test (2) of a 47-ft-span bridge at Indian Lake, New York, it was concluded, based on measurements of steel strain, deflection, and end rotation, that the full composite section was active in resisting live load. Nevertheless, because that structure was in good condition with no visible deterioration of the concrete, generalization of this result to all jack-arch bridges could not be supported.

TEST STRUCTURE

The test structure reported here was a jack-arch bridge constructed before 1915 to carry east-west

Engineering Research and Development Bureau, New York State Department of Transportation, Albany, N.Y. 12232.

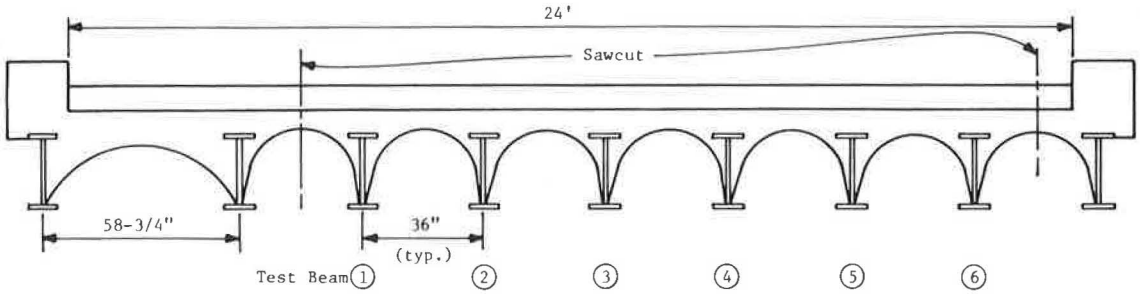

NOTE: See Figs. 2 and 7 for additional dimensions

FIGURE 1 Cross section of the test bridge.

traffic on State Route 217 over North Creek in the town of Mellenville in Columbia County, New York. The bridge's cross section (Figure 1) consisted of nine 24-in.-deep beams spaced at 36 in. except in the north exterior bay, which was 58 3/4 in. The span center-to-center of supports, which are normal to the longitudinal axis of the bridge, was 39 ft.

Condition of the bridge was poor at the time of testing. The general condition rating recommendation for the bridge, based on a May 1982 inspection, was 3. A condition rating of 3 indicates serious deterioration on New York State's scale, which runs from 1 ("potentially hazardous") to 7 ("new condition"). The lower flanges of the steel beams, which had not been encased in concrete, showed section loss due to corrosion of up to 1/4 in. at midspan locations. An HS 20 inventory rating of 4 tons was calculated for the interior beams based on reduced section properties and no composite action for the deteriorated encasement concrete.

To provide a symmetrical section for testing, longitudinal saw cuts were made (Figure 1) to provide a six-beam cross section. Original contract plans were unavailable for the bridge and it was necessary to determine properties of the steel beams from measurement on the exposed lower flanges. These measurements are shown in Figure 2. Beams 2, 4, and 5 showed only minor evidence of rust and were taken as representative of the nominal flange dimensions. These dimensions, the 24-in. section depth, and the pre-1915 construction date identified the section as a 24-in. I-section weighing 73.5 lb/ft, manufactured by Bethlehem Steel (3,p.51). Nominal dimensions for this section are also shown in Figure 2.

The deck was constructed in two pours. The first encased the beams and covered the top flanges by 3 1/4 in. to give a structural deck with a minimum thickness of 5 1/4 in. at the crown of the arches between beams. A concrete wearing surface was placed over the structural deck, varying in thickness from 8 in. at the center to 6 1/2 in. along the curb lines. Cores taken from the deck always broke into two pieces at the cold joint between the two pours. Twelve cores were taken, but only six tests could be performed. Three of these six specimens, because of their short length, were sawed and tested as 4- by 4-in. cubes. The other three, which ranged in height from 6.4 to 7.1 in. (5.65 in. in diameter), were tested as cylinders. All compression test values were factored to be representative of normal 6- by 12-in. cylinders. These tests yielded compressive strengths of 6,610 psi (average of two) for the structural deck and 6,140 psi (average of four) for the wearing surface. The strengths obtained varied considerably, ranging from 4,670 to 7,470 psi, with both extreme values from the wearing surface.

Tension test specimens were cut from the tension and compression flanges of each beam of the test bridge cross section. Average yield stress of these 12 specimens was 39.2 ksi, with a standard deviation of 3.5 ksi.

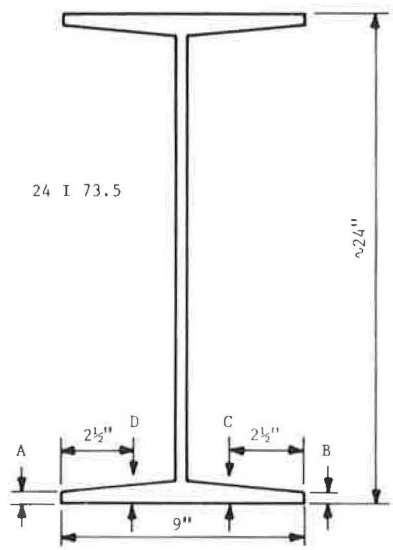

Beam	A	B	C	D
1	0.37	0.40	0.74	0.53
2	0.55	0.57	0.73	0.78
3	0.35	0.32	0.51	0.52
4	0.53	0.52	0.62	0.66
5	0.53	0.57	0.77	0.73
6	0.42	0.43	0.71	0.74
Nominal	0.51	0.51	0.74	0.74

FIGURE 2 Steel-beam cross section with dimensions.

TEST PROCEDURE AND INSTRUMENTATION

Response of the bridge to truckloads was determined before destructive testing was performed. Instrumentation for the live-load tests consisted of strain gauges bonded to the tension flanges at midspan of each steel girder.

Instrumentation for the failure test was more elaborate consisting of strain, deflection, and beam-end-rotation measurements. Test loads were applied by jacking against two load-distribution beams, each restrained by four soil anchors. Details of the instrumentation and loading system are given elsewhere (4).

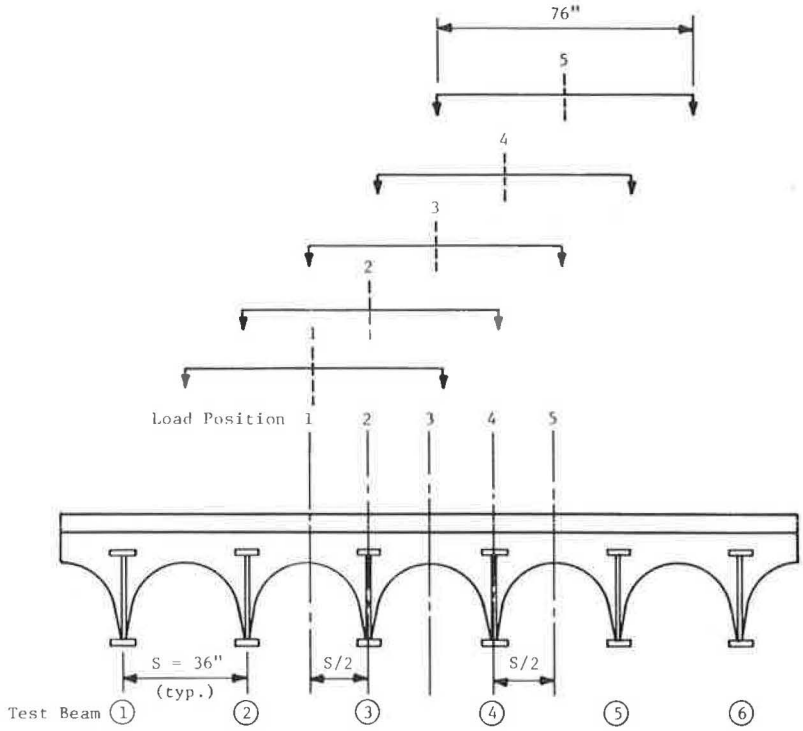

FIGURE 3 Live-load positions.

TEST DATA

Live Loads

Measured tension flange strains in microinches per inch for the load positions shown in Figure 3 are given in Table 1. These values are averages of at least three replicates of the loading. The truck in these tests produced a theoretical simple-beam bending moment at the instrumented section of 339.3 kip-ft, in contrast to the AASHTO HS 20 moment of 432.1 kip-ft for this span. Because the measurements were made with the same test vehicle, total moment in the cross section is constant. The results show a trend toward increasing total strain as the load moves toward Beam 6. This trend may result from differences in individual beam section moduli or may be simply the result of random error.

TABLE 1 Tension Flange Strain for Live Loads

	Strain (μin./in.) at Load Position				
Beam	1	2	3	4	5
1	46	35	27	20	14
2	47	45	33	28	20
3	42	44	43	44	37
4	36	43	43	44	48
5	22	29	38	43	48
6	19	27	37	46	63
Total	212	223	221	225	230

Failure Tests

Average tension and compression flange strains for each beam and load increment are given in Table 2. These are strains due to the test load only. Total strain is the sum of these values and dead-load strain. When yielding occurs, strains on opposite edges of a flange diverge, and averaging no longer provides a legitimate indication of true strain. It might be expected that this point could be predicted by simply subtracting estimated dead-load strain from yield strain to give test-load strain at the commencement of yielding. Following this procedure, expected test-load strain at first yield would be 1,060 μin./in. (1,370 - 310). The existence of residual stresses, however, introduces a further complication into the analysis. Thus, bottom flange strain averages are reported up to maximum test-load strains of from 320 to 960 psi. Averages were not taken, and no value was reported when the range of the two strains exceeded 10 percent of the average. Individual measured strains for each gauge are given elsewhere (4).

Midspan deflection for each beam is given in Table 3. Deflection at high loads exceeded the range of the displacement measuring devices. A plot of deflection versus load in Figure 4 indicates a bilinear relationship, with the break at a load of about 150 kips. Deflection at failure could not be determined, but permanent set after the load was removed exceeded 6 in. The transverse pattern of deflections was irregular (Figure 5), but this pattern was maintained throughout the range of applied loads.

End rotations measured at the east and west ends of Beams 2 and 5 are shown in Table 4 and Figure 6. It should be noted that end rotations are quite small for loads less than 150 kips but increase rapidly from that point. Total relative displacement of the abutments with respect to the beams was about 1 in. at maximum load. For loads of less than 200 kips, readings indicate that the abutments had moved toward each other by less than 0.2 in.

At maximum load, a failure plane in the slab at the interface of the structural deck and the wearing surface was evident. Although analysis of the test data (as described in the next section) indicates that these slab elements act compositely at low and

TABLE 2 Average Flange Strain

Run	Line Load (kips)	Beam Load (kips)	Strain (μin./in.) at Beam 1 Top	1 Bottom	2 Top	2 Bottom	3 Top	3 Bottom	4 Top	4 Bottom	5 Top	5 Bottom	6 Top	6 Bottom
1	0	0.0	0	0	0	0	0	0	0	0	0	0	0	0
2	10	1.7	-1	15	-15	23	-4	22	-7	25	-7	23	-7	27
3	39	6.5	-33	97	-59	102	-35	120	-41	119	-44	104	-47	118
4	70	11.7	-71	221	-94	221	-75	427	-86	297	-85	241	-93	275
5	-2	-0.2	5	18	-3	9	4	216	1	46	2	45	1	51
6	68	11.3	-78	260	-106	252	-84	490	-96	338	-95	293	-97	327
7	104	17.3	-120	446	-147	399	-131	933	-144	521	-140	508	-145	559
8	13	2.2	-12	39	-19	42	-14	44	-20	48	-18	41	-15	41
9	26	4.3	-20	73	-32	74	-28	86	-35	97	-30	78	-26	83
10	39	6.5	-36	110	-52	112	-43	122	-47	132	-41	112	-40	122
11	52	8.7	-51	151	-69	156	-54	175	-63	185	-59	160	-55	173
12	65	10.8	-62	193	-81	197	-66	218	-76	236	-72	202	-70	222
13	78	13.0	-73	232	-94	234	-76	261	-86	280	-83	240	-80	268
14	91	15.2	-87	277	-109	276	-92	310	-109	336	-103	289	-105	315
15	104	17.3	-101	318	-125	317	-105	362	-120	384	-114	328	-115	366
16	114	19.0	-118	NA	-146	367	-123	NA	-139	440	-133	391	-134	425
17	130	21.7	-130	NA	-162	419	-139	NA	-152	504	-148	513	-153	520
18	143	23.8	-147	NA	-185	488	-167	NA	-182	NA	-176	727	-170	630
19	153	25.5	-168	NA	-211	545	-201	NA	-206	NA	-198	961	-196	722
20	163	27.2	-193	NA	-230	NA	-232	NA	-242	NA	-229	NA	-227	NA
21	179	29.8	-204	NA	-236	NA	-280	NA	-274	NA	-278	NA	-292	NA
22	195	32.5	-241	NA	-274	NA	-332	NA	-332	NA	-338	NA	-364	NA
23	202	33.7	-268	NA	-303	NA	-378	NA	-372	NA	-371	NA	-414	NA
24	218	36.3	-309	NA	-335	NA	-428	NA	-433	NA	-445	NA	-493	NA
25	231	38.5	-323	NA	-370	NA	-478	NA	-480	NA	-506	NA	-568	NA
26	244	40.7	-367	NA	-422	NA	-547	NA	-562	NA	-609	NA	-676	NA
27	254	42.3	-391	NA	-454	NA	-596	NA	-624	NA	-689	NA	-771	NA
28	267	44.5	-434	NA	-520	NA	-676	NA	-764	NA	-835	NA	NA	NA
29	280	46.7	NA	NA	-633	NA	-804	NA	NA	NA	NA	NA	NA	NA
30	296	49.3	NA	NA	-795	NA	-962	NA	NA	NA	NA	NA	NA	NA
31	299	49.8	NA	NA	NA	NA	NA	NA	NA	NA	NA	NA	NA	NA
32	299	49.8	NA	NA	NA	NA	NA	NA	NA	NA	NA	NA	NA	NA
33	20	3.3	NA	NA	NA	NA	NA	NA	NA	NA	NA	NA	NA	NA

Note: Divergence of two flange gauges unacceptably large; NA indicates no average taken.

intermediate load levels, it would be incorrect to include the wearing course in calculation of ultimate capacity.

DATA ANALYSIS

The primary objective of this study was to obtain data useful in developing a load-rating procedure.

TABLE 3 Deflection

Line Load (kips)	Midspan Deflection (in.) at Beam 1	2	3	4	5	6
10	0.015	0.018	0.018	0.016	0.017	0.015
39	0.098	0.106	0.110	0.107	0.115	0.062
70	0.212	0.223	0.228	0.220	0.237	0.145
0	0.002	0.007	0.013	0.015	0.007	0.033
68	0.235	0.246	0.250	0.242	0.263	0.186
104	0.367	0.384	0.392	0.378	0.409	0.302
13	0.040	0.030	0.040	0.040	0.050	0.020
26	0.070	0.070	0.080	0.080	0.090	0.050
39	0.110	0.100	0.110	0.120	0.130	0.100
52	0.160	0.150	1.160	0.150	0.180	0.120
65	0.200	0.190	0.210	0.210	0.230	0.140
78	0.240	0.230	0.250	0.250	0.280	0.200
91	0.280	0.270	0.300	0.300	0.330	0.220
104	0.330	0.310	0.340	0.340	0.380	0.260
114	0.380	0.360	0.400	0.400	0.440	0.320
130	0.450	0.420	0.460	0.460	0.500	0.350
143	0.530	0.500	0.550	0.540	0.590	0.420
153	0.610	0.570	0.630	0.620	0.670	0.420
163	0.710	0.660	0.730	0.720	0.770	0.540
179	0.830	0.780	0.880	0.850	0.910	0.620
195	0.960	0.900	1.020	0.980	1.060	0.730
202	1.110	1.030	1.170	1.120	1.210	0.850
218	1.280	1.160	1.330	1.270	1.370	0.960
231	1.460	1.280	1.510	1.400	1.530	1.130
244	1.670	1.370	1.690	1.490	1.680	1.370

Two types of behavior--composite action between the steel and concrete and moment restraint at the supports--would result in an enhancement in strength estimates of jack-arch bridges. Refinements in the estimates of live-load distribution would also be beneficial. The data analysis has been directed to quantifying these forms of behavior.

Effective Section

The effective section resisting load can be determined from the beam-flange strain data obtained during the failure test. The initial approach to defining the effective section assumed full composite behavior and determined an effective modular ratio based on the cross section assumed and the measured tension and compression flange strains. This approach was abandoned when it became clear that, even with a 5-in. deck thickness, comparisons of the analytical and experimental neutral axis locations were inconsistent, regardless of the value assumed for the modular ratio. An approach was required that used the physical and geometric properties of the section tested. The process used conceptualizes the total bending moment carried as the sum of the moments resisted by the steel beam and slab individually, plus a couple formed by the equal and opposite internal thrusts acting at the centroids of these elements. Figure 7 shows these forces and invariant slab dimensions. The arch radius changed 4.5 in. below the crown, and concrete below this level was ignored. In addition to assuming a value for the elastic modulus of the concrete (n = 8), it is assumed that curvature of the beam and slab are equal and that the beam thrust calculated from the measured strains is resisted by an equal but opposite thrust in the slab as required for equilibrium. This latter as-

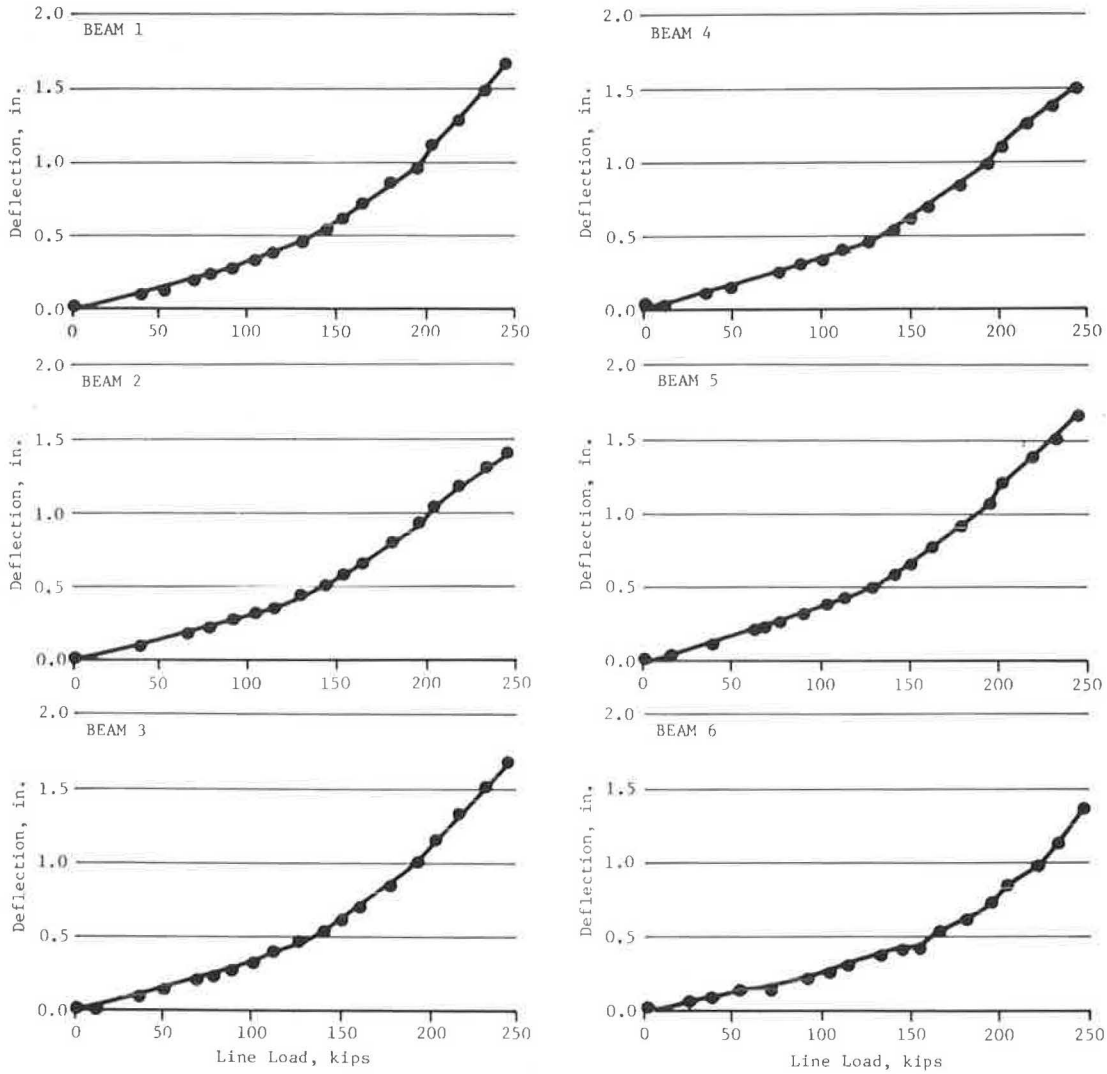

FIGURE 4 Midspan deflections.

sumption is equivalent to assuming that the relative measured displacements of the beams with respect to the abutments did not result in an induced axial beam force. In contrast to ordinary design practice, some tension (for this structure up to 500 psi) has been permitted in the concrete. The appropriate relationships are developed elsewhere (4). From this analysis an effective moment of inertia and the total resist-

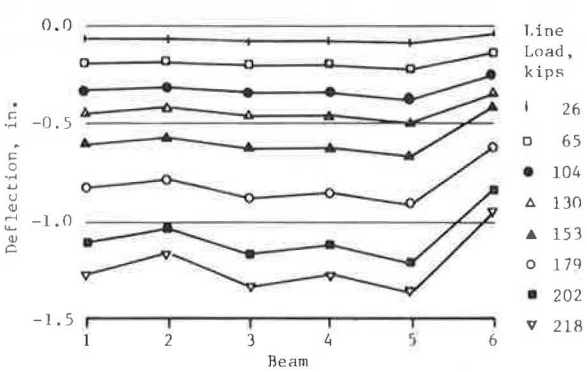

FIGURE 5 Transverse deflection pattern.

TABLE 4 End Rotation

Line Load (kips)	Rotation (radians x 10^3)			
	2E	2W	5E	5W
13	0.000	-0.050	-0.050	-0.050
26	0.050	-0.050	-0.100	0.050
39	0.250	-0.100	-0.050	0.250
52	0.500	-0.050	-0.100	0.550
65	0.750	0.150	-0.050	0.750
78	1.000	0.500	-0.250	1.050
91	1.250	0.650	-0.300	1.300
104	1.600	0.900	0.650	1.550
114	1.750	1.150	0.550	1.950
130	2.250	1.450	0.450	2.350
143	2.550	1.800	0.250	2.950
153	3.250	2.100	1.500	3.350
163	3.750	2.550	1.300	4.050
179	4.450	3.500	1.050	4.850
195	5.450	4.050	2.500	5.750
202	6.500	4.750	2.200	6.750
218	7.700	5.600	3.750	7.950
231	9.050	6.550	4.650	9.150
244	10.650	8.250	5.150	10.750
254	12.050	9.150	6.050	NA
267	14.450	12.900	7.650	14.250
280	18.950	16.350	10.000	18.550
296	24.050	21.900	13.250	23.150
299	30.450	26.350	26.050	29.650
299	31.850	24.200	39.400	43.450

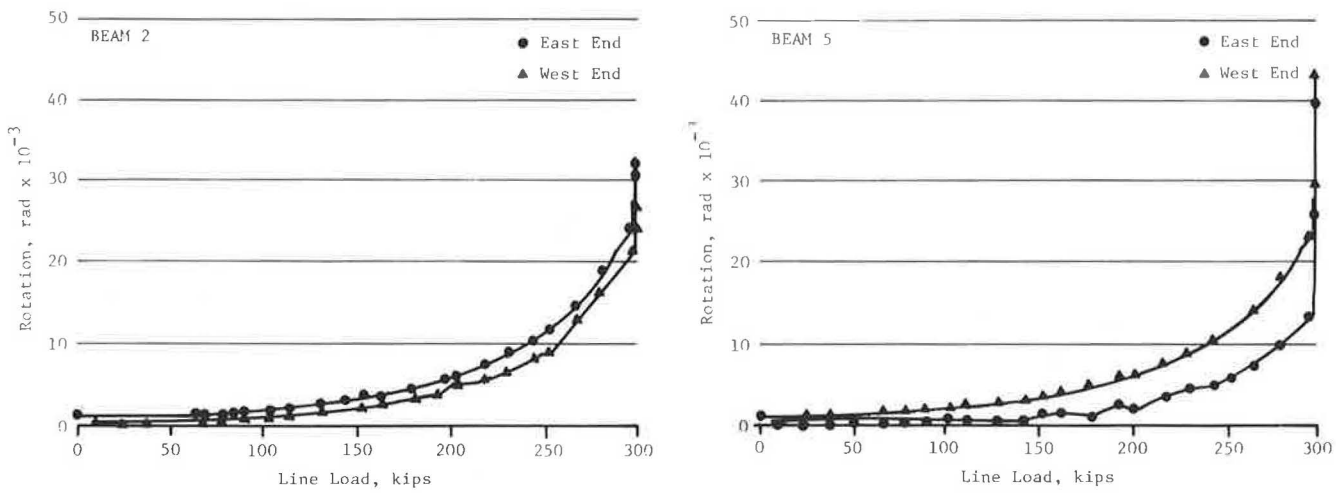

FIGURE 6 End rotation related to line load.

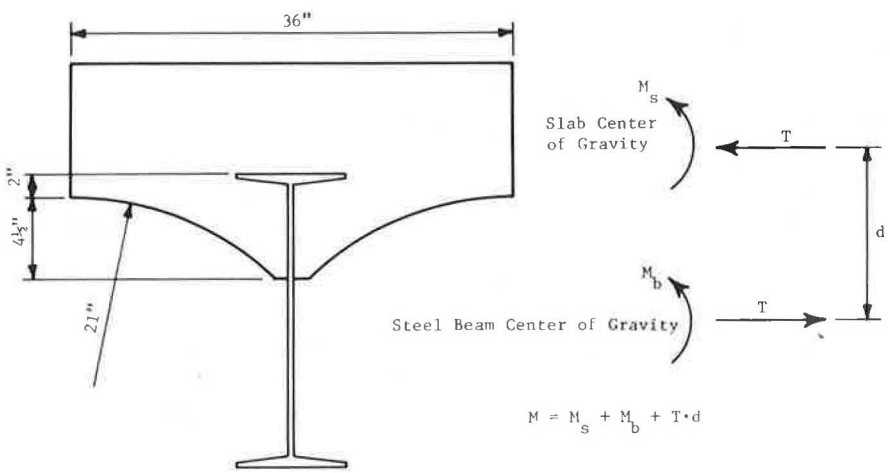

FIGURE 7 Effective section.

ing moment at the measured strain level are obtained. This analysis is, of course, only valid for elastic strains.

Data from the first two loadings (Runs 1 through 7) gave erratic results that are not believed to be representative of true structural behavior and thus were excluded from the reported results:

	Beam Properties			
Beam	Slab t (in.)	Flange t (in.)	I_{eff} (in.^{4})	α
1	11.750	0.62	4,800	0.545
2	12.375	0.74	5,010	0.439
3	13.375	0.50	4,800	0.466
4	13.250	0.63	5,180	0.475
5	13.250	0.74	5,510	0.477
6	12.500	0.71	5,350	0.540

These values are based on data from the final loading of the bridge up to the load providing consistent strains on the edges of the tension flange (104 kips). The effective inertia can be expressed as

$$I_{eff} = \alpha I_c + (1 - \alpha) I_{nc}$$

where the subscripts eff, c, and nc stand for effective, composite, and noncomposite, respectively.

The results of this analysis can also be used to determine the degree of end restraint for this bridge. This is done by comparing static midspan bending moment with estimated bending moment from the strain analysis. This comparison is shown in Figure 8 in which it can be seen that the experimental moments are linear with increasing load and are always less than the static values. Based on this result, the end moment is estimated to be 30 percent of the fixed-end value during the elastic portion of the failure test.

Live Loads

Tension flange strains measured during live-load testing were converted to bending moment using the effective section properties determined from the strain analysis just described. These experimental values were compared with the results from a planar-grid analysis. For this analysis the bridge was assumed to be fixed ended despite the findings from the failure test. It is believed that end moment restraint was partly destroyed during the first increments of the failure loads. It should be noted that the midspan bending moment (assuming a simply supported beam) was only 339 kip-ft--a value exceeded between the first and second failure load increments. In addition, it has been previously noted that the

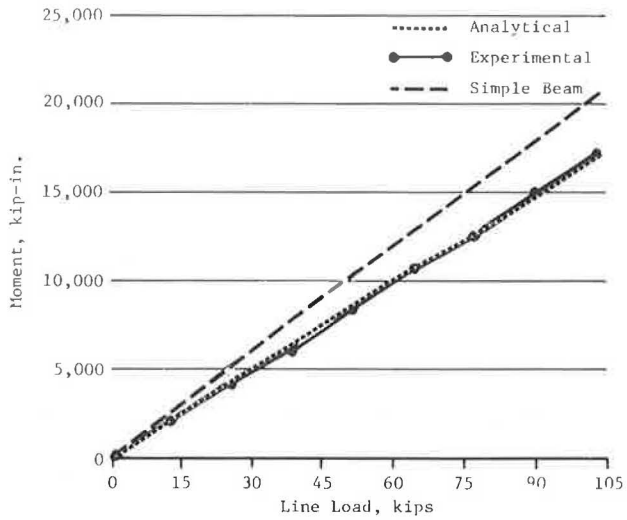

FIGURE 8 Analytical and experimental moments.

structure's behavior under the first increments of failure load was erratic, which indicated a change in behavior.

Figure 9 shows experimental and analytical midspan bending moments for each load position. In general, the analytical values overestimate the experimental moments, and the differences are more prominent on the fascia beams. The total experimental moment for each load position (Figure 10), which theoretically should be constant, varies with load position. Although this variation is not large, it is systematic: the total moment increases as the load position moves across the width of the structure.

Live-load distribution coefficients can be obtained by dividing the beam moments by total moment at the cross section for a particular load position. This structure was so narrow, however, that meaningful values could not be calculated because only one vehicle could be placed at a time.

Failure Loads

End rotation and centerline deflection data are shown in Figures 11 and 12, with calculated values based on the elastic properties determined from the strain results. Values are shown for a simple span and a span restrained with end moments equal to 30 percent of the fixed-end values. For both deformations the restrained solution compares well with the experimental values for lower loads, which supports the findings for effective inertia and end restraint from the strain analysis. Both deformations increase rapidly at a line load of about 150 kips, indicating the initiation of inelastic behavior.

Elastic predictions of beam deflections do not compare well with measured values on an individual basis. Figure 13 shows this comparison for two levels of line load. In general, the analysis overestimates the measured values. Transverse variations in experimental deflection are not reflected in the analytical results, which suggests that the observed variation is a consequence of loss of transverse rather than longitudinal stiffness. Data are insufficient on the possible degradation of concrete properties with location in the structure to make a specific estimate of this effect. It should be noted that transverse variations are small with respect to average values.

Deflection comparisons could be improved by increasing the beam stiffnesses, the amount of end

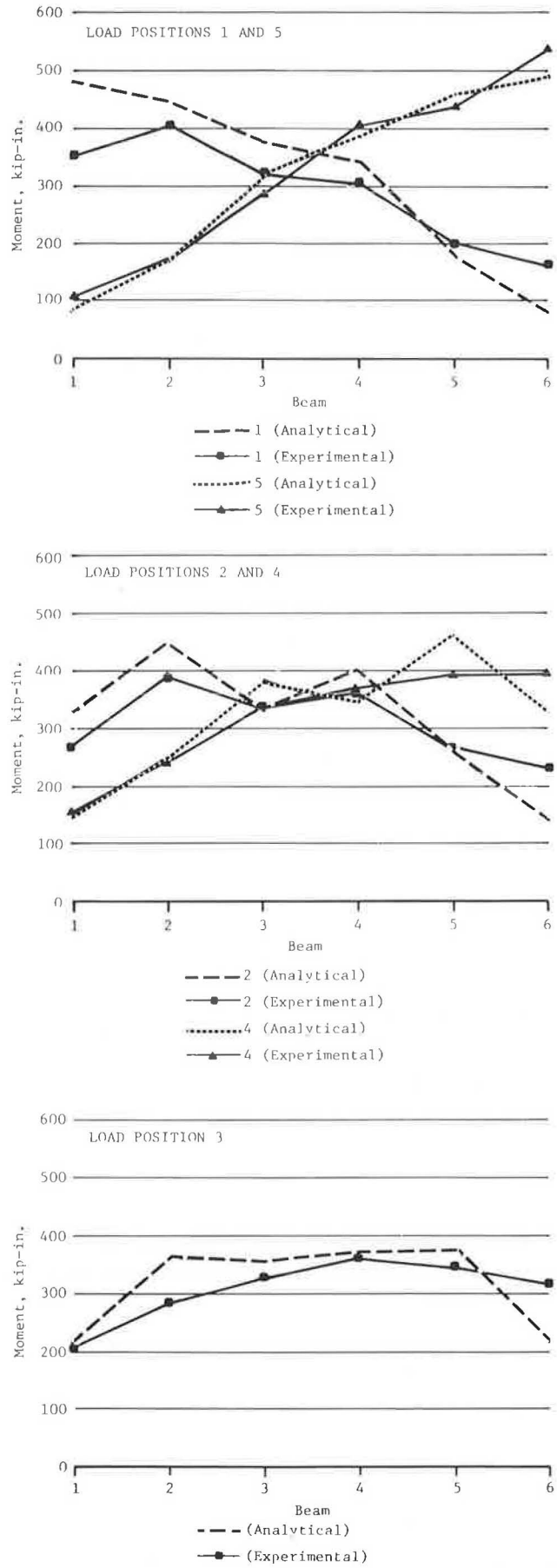

FIGURE 9 Analytical and experimental live-load moments.

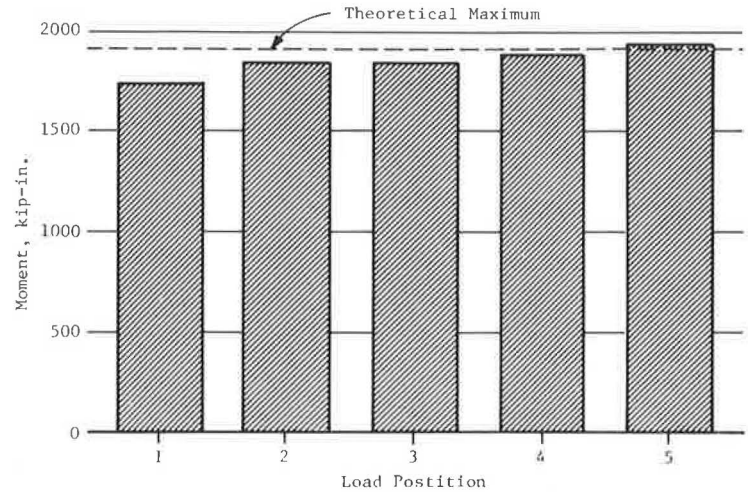

FIGURE 10 Total live-load moments.

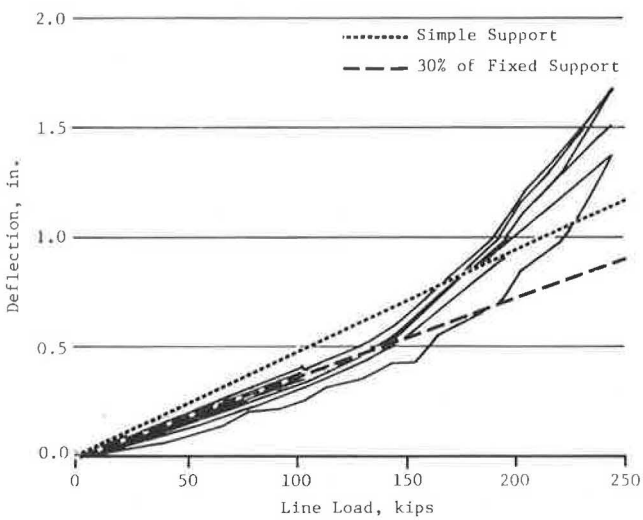

FIGURE 11 Line load related to deflection.

restraint, or both, but such adjustments are not supported by the strain data. The analytical-to-experimental bending moment comparisons (Figure 14) also show greater transverse variation in the experimental results than are predicted analytically, although these variations are not as pronounced as for deflection. Because the total experimental and analytical moments compare satisfactorily (Figure 8) it is clear that changes in the magnitude of end restraint are unwarranted, because this would have a direct effect on the moment comparisons. Refinements in section properties would have only a minor influence on the strain-to-moment conversion (increasing the inertia would result in increased moment) but would tend to reduce transverse variation in the analytical results. More important, increases in section inertia can only be achieved by decreasing the assumed value for the modular ratio, and the

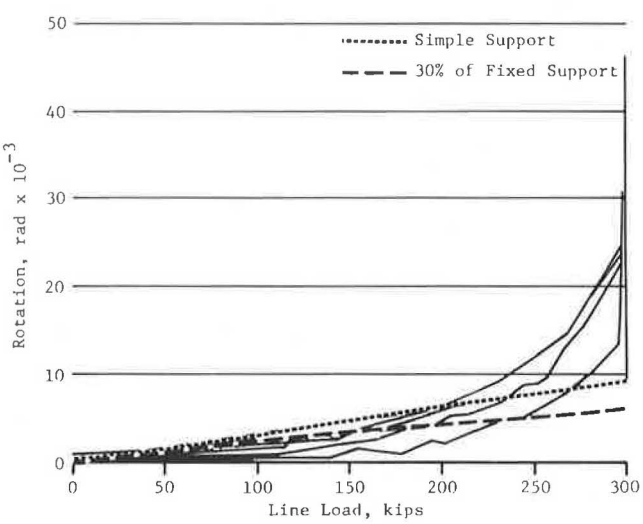

FIGURE 12 Line load related to end rotation.

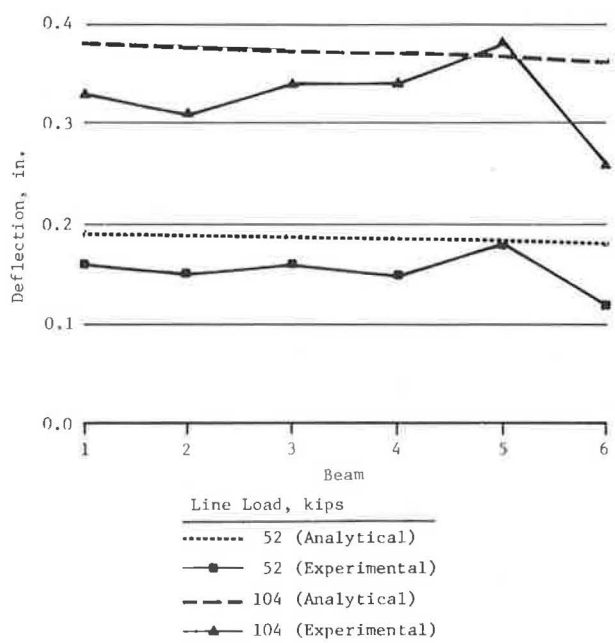

FIGURE 13 Midspan displacement.

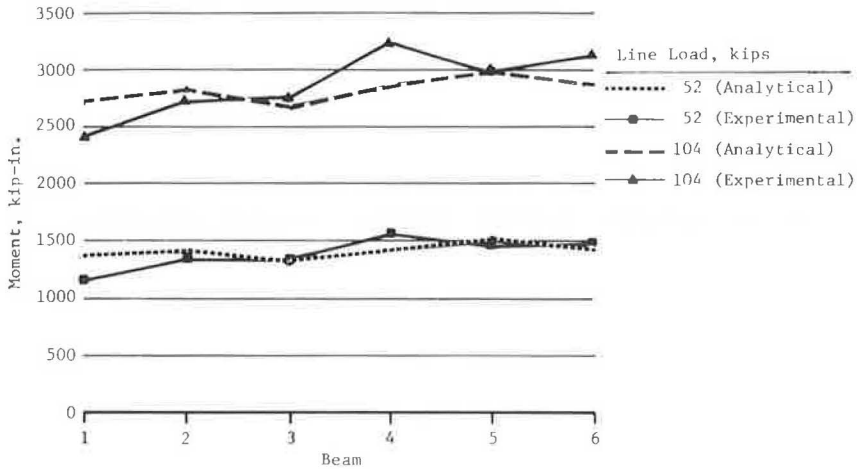

FIGURE 14 Midspan bending moment.

value assumed (n = 8) is judged to be the smallest reasonable value for concrete in this condition. Overall comparison of deflection and end rotation data with the analytical estimates supports the validity of the data analysis procedures used for converting measured strain to bending moment and estimating the effective moment of inertia.

Postelastic behavior of this structure has not been investigated in detail because of the lack of full strain data. Delamination of the deck at the interface between the structural and wearing-surface concrete was visible at the maximum load. Because of this delamination the wearing surface should be ignored when estimating the failure load. It should be noted that the maximum load applied to this structure was twice the elastic limit load of 150 kips.

APPLICATION TO LOAD RATING

The procedures used in this study are theoretically correct and produce results that are consistent with observed behavior. Nevertheless, these techniques bear little resemblance to procedures used in conventional design or load-rating practice. It would be unrealistic to expect that a procedure requiring calculation of an effective partly composite section would be received with enthusiasm by engineers working in a production environment. In addition, some criteria would have to be established for maximum allowable concrete tension to permit determination of the effective section depth.

A conventional analysis would compute a tension flange section modulus based on a fully composite section, with tension concrete ignored. For this structure the tension flange strains based on this section and the experimentally determined beam moments overestimate the measured strain by only 3 percent. Despite this good comparison, it should be realized that stiffness of the composite section is at least 25 percent greater than the effective section determined from the measured strains. Nevertheless, estimates of induced stress based on properties of the composite section produce reliable estimates of the true values. This result was also found for the Indian Lake structure tested earlier (2).

The test results show that end restraint equivalent to 30 percent of the fixed-end amount was active for loads of less than 150 kips (equivalent design load with impact = 2.7 HS 20 trucks). For the Indian Lake bridge it was found that full fixity was present for loads less than the service load. Thus estimates of structural capacity that ignore these effects will be conservative. Generalization of the degree of composite action or the magnitude of end fixity is not possible now, and it is not likely that a technically defensible generalization could ever be produced regardless of the number of bridge tests performed.

Load ratings for the Mellenville bridge have been calculated for the H 15, the HS 20, and the three typical legal load types specified by AASHTO (5,p.50). Those ratings are based on the properties of Beam 3--the most deteriorated beam in the cross section. No end fixity was assumed in these computations. Load-rating factors (load-factor method using properties of Beam 3) for each of these loadings were as follows:

	Rating Factors		
Vehicle	Inventory	Operating	Serviceability
H 15	1.55	2.58	3.83
HS 20	0.92	1.53	2.27
Type 3	1.26	2.11	3.12
Type 3S2	1.26	2.11	3.12
Type 3-3	1.45	2.42	3.58

Multiplying the rating factor times the rating vehicle weight gives the structure's load capacity for the specific load type. Note that although the inventory rating factor for the HS 20 load is slightly less than unity, posting of the structure would probably not be necessary in view of the ample operating and serviceability ratings.

CONCLUSIONS

Based on the results of failure tests on two jack-arch bridges, the following conclusions can be drawn:

1. Assuming full composite behavior results in conservative estimates of structural behavior.
2. Significant end fixity exists under service load. The effect of this moment restraint is to reduce the midspan bending moment estimated for a simply supported beam.
3. It is not now possible to generalize the prediction of the degree of end fixity to other structures. The source of end fixity for the test structure has not been determined.
4. The test structure remained elastic for loads producing bending moments equivalent to 2.7 HS 20 design vehicles (including impact).

5. A load rating based on the most deteriorated member in the cross section indicates that this structure could have been used safely without posting.

ACKNOWLEDGMENTS

Robert J. Kissane, Civil Engineer II (Physical Research), assisted in planning this test and was responsible for supervising the field work. Wilfred J. Deschamps, Everett W. Dillon, Michael D. Gray, Joel W. Miller, Samuel P. Morris, and Frank P. Pezze installed instrumentation and assisted in monitoring the structure's response to load. Brian Johnson, Student Intern, aided in the data reduction and structural analysis. The research reported was conducted in cooperation with the Federal Highway Administration, U.S. Department of Transportation.

REFERENCES

1. Load Test: Route 30A over Canal. BIN 4021420. Memorandum of May 19, 1983, from W.C. Burnett, Engineering Research and Development Bureau, to E.V. Hourigan, Structures Design and Construction Division, New York State Department of Transportation, Albany.
2. D.B. Beal. Failure Tests of a Jack Arch Bridge. Research Report 110. Engineering Research and Development Bureau, New York State Department of Transportation, Albany, Feb. 1984.
3. Iron and Steel Beams: 1873 to 1952. American Institute of Steel Construction, New York, N.Y. 1953.
4. D.B. Beal. Load Capacity of a Jack-Arch Bridge. Research Report 129. Engineering Research and Development Bureau, New York State Department of Transportation, Albany, Dec. 1985.
5. Manual for Maintenance Inspection of Bridges 1983. AASHTO, Washington, D.C., 1983.

Publication of this paper sponsored by Committee on Steel Bridges and Committee on Dynamics and Field Testing of Bridges.